JOURNAL OF MATERIALS SCIENCE **37** (2002) 2043–2051

Surface morphologies of composites based on unsaturated polyester pre-polymer

M. VAYER, C. SERRÉ, N. BOYARD, C. SINTUREL, R. ERRE
Centre de Recherche sur la Matière Divisée, CNRS- Université d'Orléans, 1b, rue de la Férollerie, F45071 Orléans Cedex 2, France
E-mail: marylene.vayer@univ-orleans.fr

We report the study of surfaces of bulk molding compounds (BMC) based on miscible polymeric thermoset blends (TB)—unsaturated polyester, styrene and low profile additive (LPA)—containing fillers and glass fibers. In contrast to scanning electron microscopy (SEM) that identified a continuous organic layer at the BMC surface, atomic force microscopy (AFM) showed the existence of aggregates linked together to form a network at the micrometric scale. This indisputably demonstrated that phase separation took place at the surface of the BMC. The influence of TB was examined by comparing the surface morphologies of BMC and corresponding TB. Several cases were distinguished as a function of the TB composition. (1) Without LPA, the surface of the TB was continuous (no phase separation took place during curing) and the surface of BMC revealed the presence of aggregates resulting from a phase separation induced by the fillers. (2) For very low molecular weight LPA, aggregates randomly spread on islands surrounded by large holes were observed on the TB surface. These holes were shown to result from surface deformations induced by absence of shrinkage compensation. The corresponding BMC presented particles randomly spread on the surface. (3) The general case (higher molecular weight LPA) corresponded to similar TB and BMC surfaces morphologies with aggregates randomly spread on the surface. In this case, BMC roughness and morphology reflected the TB roughness and morphology. These observations led to the proposal of some considerations concerning the control of surface aspects of BMC.

1. Introduction

Bulk molding compounds (BMC) are composite materials based on organic thermoset systems—15/25 wt% of unsaturated polyester (UP) crosslinked by styrene (ST)—containing mineral fillers and reinforcement fibers. This kind of polymeric composites is widely used for automotive and plumbing pieces because of good surface finish (i.e. gloss or smoothness) and dimensional stability. To achieve this goal, low profile additives (LPA) such as poly(vinylacetate) and poly(methylmethacrylate) are used to prevent crosslinking shrinkage [1] and to improve the surface quality. However the mechanisms of this improvement are not clearly identified and despite intensive industrial production, few academic works deal with thermoset surfaces (either characterization or influencing parameter). Some parameters like fillers and fibers volume [2], molding processing parameters—molding pressure and temperature—are also determinant for a good surface aspect [3] but their contributions are difficult to evaluate. The BMC surface is consequently far from being completely under control.

The volume morphology of these crosslinked polymeric systems is however largely documented [4]. This morphology after curing depends on the initial miscibility of the ternary UP/LPA/ST thermoset blend (TB) [5] and its evolution during curing. For initially miscible systems, the morphology is generally described as a co-continuous structure with microparticles of cured UP connected in a macro-network, and a continuous LPA phase surrounding these microparticles [6]. Micropores are also pointed out in the structure and generally account for the polymerization shrinkage compensation. However, the mechanism of formation of these micropores (thermal expansion of LPA [7] or stress relaxation [8]) and even their localization (interfacial region between crosslinked UP and LPA phase [9] or inside the LPA phase) are still controversial.

Concerning the surface, preliminary works based on scanning electron microscopy and XPS analysis [10] have demonstrated that the surface of BMC materials molded by compression was composed of an organic layer. Mineral fillers and glass fibers were shown to be deeper localized beneath the surface (>0.4 μm), the glass fibers in a parallel position to the plan of the surface [10]. In this paper, BMC surfaces were explored at nanometrical scale by atomic force microscopy which has been recently successfully used to investigate the

morphology of thermoset materials [11]. The corresponding TB surfaces were also studied and compared. LPA used in this study were low molecular weight saturated polyester (highly compatible with UP), rarely considered either in the industry or even academically.

2. Experimental

2.1. Materials

The polymeric thermoset blends (TB) were composed of (i) an unsaturated polyester prepolymer (UP) (ii) a curing agent (styrene referred in the text as ST) (iii) a polymerization initiator (ter-butyl perbenzoate; 1 wt%) (iv) a low profile additive (LPA). Different LPA (saturated polyester, and urethane modified saturated polyester) were employed (Table I) at various compositions (Table II).

BMC samples were composed of (i) 18 wt% of TB (ii) internal mold release agent (calcium stearate; 1 wt%; particles diameters ranging from 2 to 13 μm) (iii) mineral fillers (calcium carbonate; 62 wt%; particles diameters ranging from 1 to 10 μm) (iv) glass fibers (20 wt%; 12 μm wide and 3 mm long). In the BMC, composition of the organic blend was the only fluctuating parameter.

BMC plates (120 × 250 × 3 mm) and TB cylindrical samples (Ø 50 × 4 mm) were molded by compression using a Derek press in a stainless steel mold. Special attention was paid to the level of polishing of the female part of the mold since the BMC roughness is limited by the mold roughness (5 nm) [12]. The polished female part was heated at 150°C and the punching die at 135°C. Pressure applied on composite was 10 MPa and the curing time was 100 seconds.

2.2. Instrumentation

Scanning electron microscopy (SEM) was carried out on a Hitachi S4200 device combined with an Oxford analyzer controlled by Link Isis software. The electron gun was equipped with a field emission electron source and was operated at 1–2 keV.

TABLE I UP and LPA characteristics

Name	Characteristics
Unsaturated prepolymer UP	Unsaturated polyester: maleic anhydride-propylene glycol $M_n = 1250$ g·mol^{-1} $M_w = 6790$ g·mol^{-1}
Low profile additive	Saturated polyester: adipic acid-propylene glycol-ethylene glycol
LPA-1265	$M_n = 1265$ g·mol^{-1} $M_w = 2970$ g·mol^{-1}
LPA-1960	$M_n = 1960$ g·mol^{-1} $M_w = 3930$ g·mol^{-1}
LPA-2250	$M_n = 2250$ g·mol^{-1} $M_w = 4830$ g·mol^{-1}
LPA-2685	$M_n = 2685$ g·mol^{-1} $M_w = 6790$ g·mol^{-1}
LPA-U	Urethane modified saturated polyester: adipic acid-propylene glycol-ethylene glycol-diisocyante $M_n = 5300$ g·mol^{-1} $M_w = 13300$ g·mol^{-1}

Atomic force microscopy (AFM) was carried out in air using Nanoscope III from Digital Instruments Corporation in the tapping mode. The piezo scanner was able to scan with a horizontal range of 150 μm and a vertical range of 7 μm. Microfabricated Si 120 μm long cantilevers with integrated Si pyramidal tip (10 to 15 μm height) were used. Resonance frequency was in the range 300–400 kHz. Vertical and lateral resolutions were less than 1×10^{-3} μm.

Analyses (SEM, AFM) were performed on the sample side in contact with polished female part of the mold, without any further preparation in the case of the AFM observation and with a carbon-coating in the case of the SEM analyses.

Volume shrinkage (V_s) and porous volume (μ) percentages were estimated by measuring sample density by immersion in pure water. V_s and μ are then given by the following relations:

$$V_s = \frac{d_{\text{exp}} - d_1}{d_1} \times 100 \qquad \mu = \frac{d_2 - d_{\text{exp}}}{d_2} \times 100$$

where d_1 was the density of the sample before curing, d_2 the theoretical density of the sample after curing calculated from the density and the weight fraction of each constituent of the sample and d_{exp} the experimental density of the sample measured by immersion in pure water.

Average surface roughness (R_a) was estimated thanks to AFM images by the relation

$$R_a = \frac{1}{N^2} \sum_{N*N} \left| Z - \bar{Z} \right|$$

where N^2 was the image pixels number, Z was the current height and $\bar{Z}$ was the average roughness.

3. Results and discussion

3.1. Surface morphology of BMC imaged by SEM and AFM

When observed by SEM, the surface of a BMC appeared to be continuous and homogenous, even at high magnification (Fig. 1). The obtained images were principally formed by the secondary electrons emerging from the surface layers (maximum 0.02 μm) with a contribution of the backscattered electrons, which intensity and production depth depended on the accelerating voltage. This latter contribution was lowered by decreasing the acceleration voltage (at 2 keV the incident penetration depth of electrons was 0.6 μm and the corresponding information depth was limited to 0.05 μm [10]. Under these conditions, the SEM images corresponded only to the surface layers [13, 14].

Considering the organic nature of this surface layer, SEM images constituted an unexpected behavior. A morphology resulting from a phase separation (i.e. with particles linked together to form a network) would be

TABLE II Thermoset blend (TB) compositions

Compositions	1	2	3	4	5	6	7
LPA type	–	LPA-2685	LPA-2250	LPA-1960	LPA-1265	LPA-2250	LPA-U
UP/LPA/ST (wt%)	60/0/40	49/18/33	49/18/33	49/18/33	49/18/33	47/12/41	47/12/41

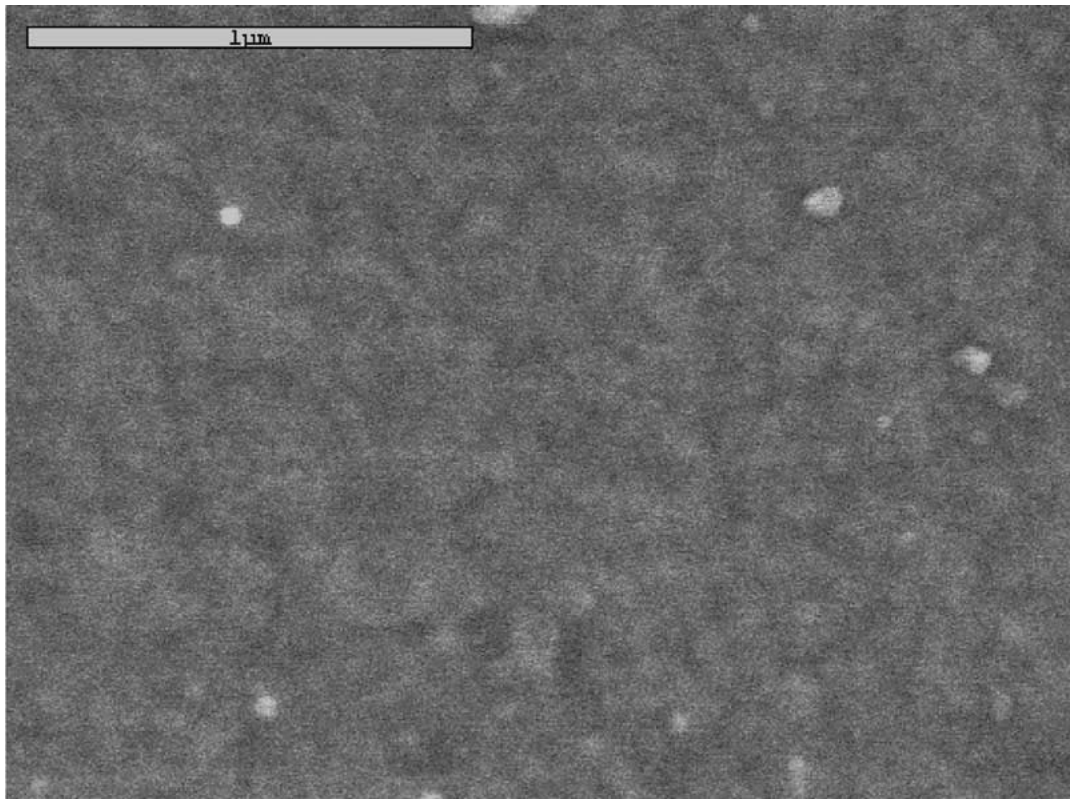

Figure 1 SEM image of a BMC surface at 2 keV. Magnification × 50000.

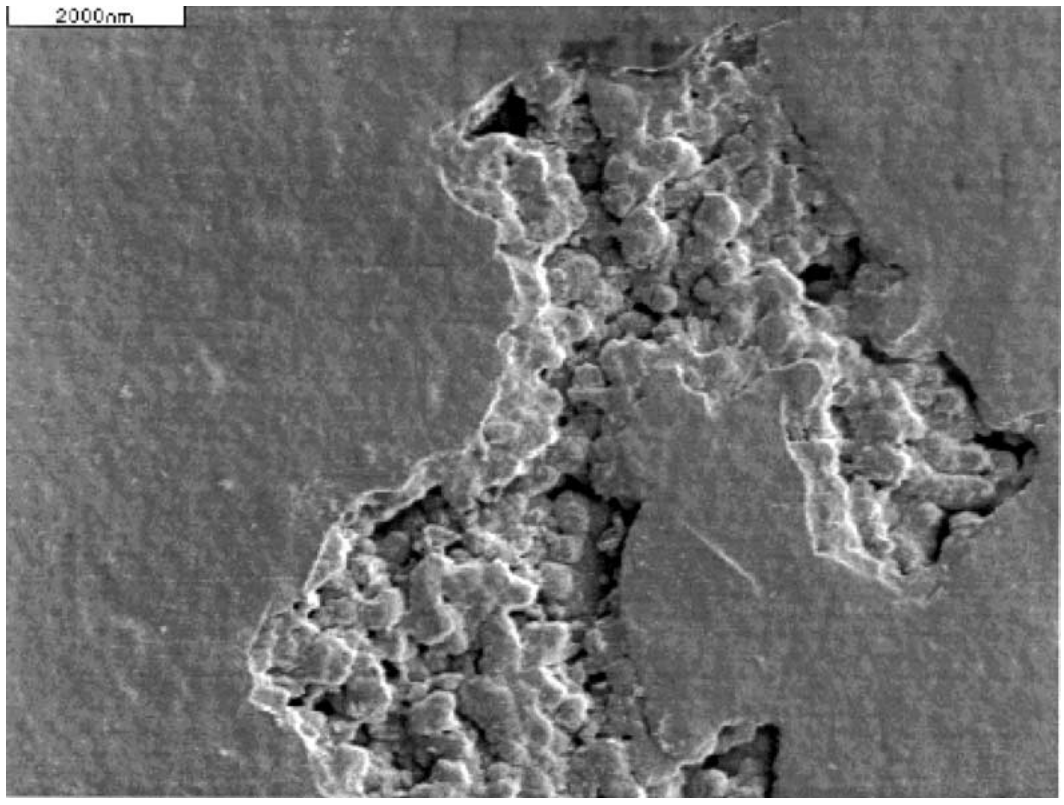

Figure 2 SEM image of a BMC surface defect at 1 keV. Magnification × 13000.

indeed expected, as it is usually reported for TB containing LPA. However, the presence of this continuous layer on BMC surface based on other TB (UP/PVAc/ST) has been already reported in other SEM works [14]. The continuous nature of this layer has been then explained by cross-linking at the surface without any phase separation [15]. During our SEM study, peculiar attention was given to extremely rare defects due to lack of molding agent or defects of the mold. The surface layer was then pulled out in the place of these defects. Example of such phenomenon is illustrated in Fig. 2. These defects pointed out the presence of an other type of morphology originating from a phase separation beneath the surface layer.

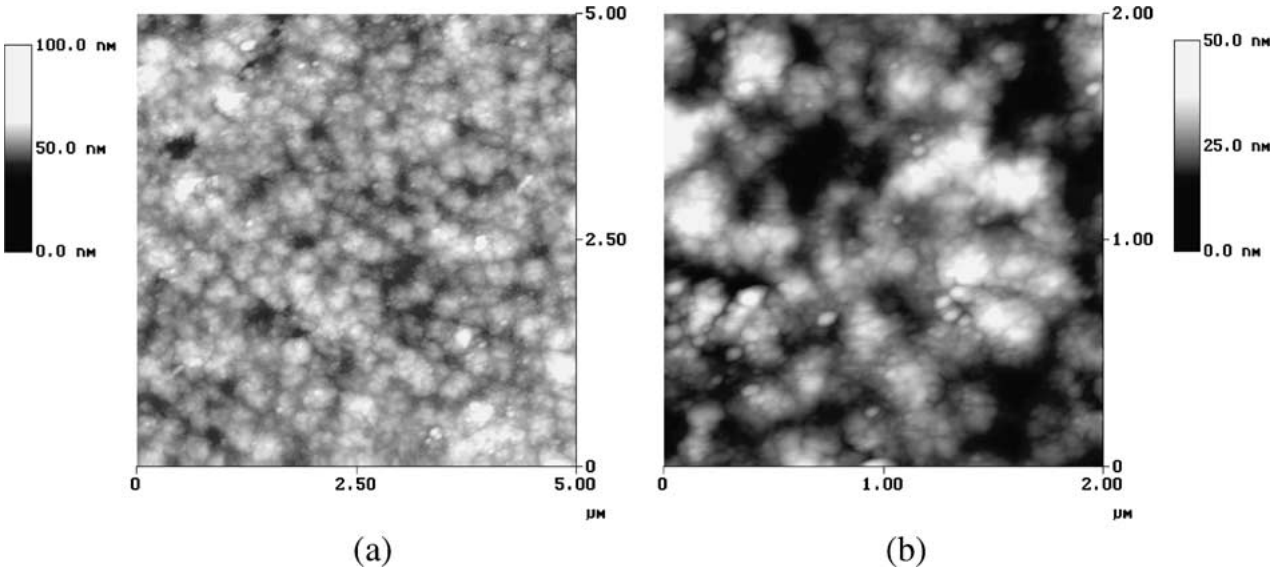

Figure 3 AFM image of a BMC surface. (a) 2*2 μm (b) 10*10 μm.

In order to precise the nature of the surface layer, we carried out an AFM study of the surface, which has been recently successfully used to investigate the morphology of thermoset organic samples [11]. In contrast to the SEM observation the AFM imaging of the surface did not revealed a continuous structure. This could be observed in Fig. 3 where the surface layer appeared to be discontinuous, and composed of aggregates (300 nm) of smaller particles (60 nm) linked together to form a bi-dimensional network. Consequently and already demonstrated in the case of thermoset blends [11] AFM imaged more precisely the surface layer than SEM did. Up to now, BMC surface layer has been seen as a continuous layer [14]. From now it has to be considered as formed with particles linked together where a phase separation takes place during the cross-linking. In this case SEM limitations could be related to the low roughness of the surface, due to the contact with the mold. This hypothesis was consistent with the fact that morphology was easily revealed by SEM when the material was highly rough (fractured sample which is a common way of samples preparation for SEM observation, or defects at surface as reported above).

3.2. Factors influencing the surface morphology of BMC

As demonstrated above, AFM constitutes a pertinent and convenient way to explore at the nanometric scale surface layer of BMC thermoset composite. Consequently, surfaces of BMC containing different LPA at various concentrations were characterized by AFM (Figs 4a, 5a, 6a, 7a, 8a, 9a, 10a). All the studied surfaces exhibited small particles linked together in aggregates. For each samples, the aggregate size and surface roughness were evaluated from the images (Table III). BMC and the corresponding TB surfaces morphologies were then compared (Figs 4b, 5b, 6b, 7b, 8b, 9b, 10b). These samples were also characterized in term of macroscopic aspect, i.e. volume shrinkage, pores volume and aspect of sample (Table IV). For the latter, a TB translucent appearance corresponded to a small pore volume, which was associated with a relatively high volume shrinkage. In contrast, a white opaque appearance was related to a large pore volume and small volume shrinkage. Concerning the BMC, all samples were opaque due to intense light scattering of the fillers.

TABLE III Comparison of some BMC properties: aggregates size, pore volume, roughness, visual appearance and volume shrinkage

BMC comp.	Aggr. size (nm) (st.dev. = 10)	μ(%) (st.dev. = 0.1)	R_a (nm) (st.dev. = 1)
1	270	0	10
2	250	3.6	6
3	290	3.4	5
4	325	3.5	8
5	270	2.5	7
6	310	2.5	8
7	–	3.9	16

In the case of samples based on cross-linked UP/ST without any LPA (composition 1), surface morphologies of the TB and the corresponding BMC (Fig. 4) were very different. For TB (Fig. 4b), a continuous morphology was observed without any particle and aggregate indicating that no phase separation took place during the cross-linking. This was expected since the binary system (UP/ST) remained miscible during the curing. This result was also consistent with the absence of pore reported in Table IV and corresponding to a high volume shrinkage. Pore formation resulted from localized stress relaxation at interfaces created during phase separation. In contrast, the corresponding BMC (Fig. 4a) exhibited a discontinuous morphology on the surface with aggregates. In this case, a phase separation took place during cross-linking, that could be attributed to the presence of fillers. Surprisingly, no pore was developed in this case in the volume indicating the formation of a highly connected polymeric network. The resulting shrinkage (0.9%) was lower than the value reported for TB (9%) because directly related to the weight fraction of TB in the BMC (fillers and fiber glass volumes were not modified during curing). However, and despite this low volume shrinkage value, compositions without

TABLE IV Comparison of some TB properties: aggregates size, pore volume, roughness

TB Comp.	Visual appearance	Aggr. Size (nm) (st.dev. = 10)	V_s(%) (st.dev. = 0.1)	μ% (st.dev. = 0.1)	R_a (nm) (st.dev. = 1)
1	Translucent	–	9.3	0	5
2	White opaque	140	5.0	2.6	10
3	White opaque	140	5.9	1.7	10
4	Cloudy translucent	140	7.3	0.6	29
5	Cloudy translucent	140	7.4	0.0	44
6	White opaque	170	6.0	3.6	12
7	Cloudy translucent	150	8.4	0.8	5

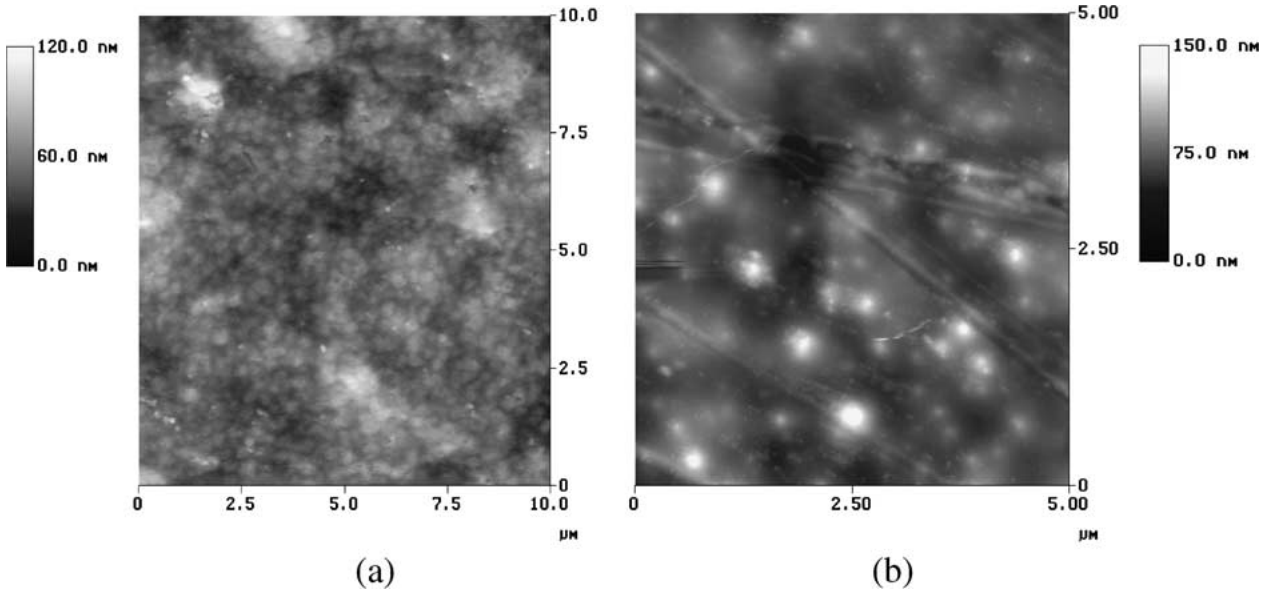

Figure 4 AFM images of (a) BMC1 surface and (b) TB1 surface.

LPA led as expected to unusable compositions for industrial applications where volume shrinkage for BMC low-profile must be less than 0.05%.

When LPA was added to the mixture, the AFM observation of the surface exhibited small particles linked together in aggregates either in the case of the TB or the BMC. Particles and aggregates were however found to be bigger on BMC surface than on TB sample surface (250/325 nm for BMC versus 140/230 nm for TB), that can be explained by a variation of the cross-linking kinetics of the outermost layer of BMC and TB. This surface morphology was the result of a phase separation induced by the LPA, which allowed the creation of pores within the samples either in the case of BMC or TB, leading to a shrinkage compensation. However, and despite a low content of polymeric phase (18 wt%), it is worth noting that the pore volume was higher in the case of the BMC samples (between 2.5 and 3.5%), leading to a high shrinkage compensation. This behavior was initiated by the presence of LPA but enhanced by the presence of fillers known for their shrinkage compensation effect.

The influence of LPA characteristics (molecular weight, amount and chemical nature) was then considered.

3.2.1. Influence of the molecular weight

The influence of the molecular weight of the LPA (with a given concentration of 18 wt%) was examined with compositions 2 to 5 corresponding respectively to $M_n = 2685$, 2250, 1960 and 1265 $g \cdot mol^{-1}$. AFM images (Figs 5–8) showed different behaviours for the BMC and the TB.

In the case of TB samples, homogeneous discontinuous structures were observed for the compositions 2 and 3 (corresponding to the higher molecular weight). Measured roughnesses were in that case about 10 nm. The lower molecular weight LPA compositions (5 and 6) exhibited aggregates randomly disposed on islands surrounded by large holes. For these latter samples, global high roughnesses were reported (29 and 44 nm) although particles and aggregates were relatively small with smooth surfaces between the holes (roughness between the holes 5 nm). These high values were thus related to the presence of this large holes at the surface that contributed to increase the global roughness. This particular behavior was explained by the absence of pore in the structure due to formation of a highly connected polymeric network during the co-polymerization. This was related to the high miscibility domain of the considered ternary blends (LPA/UP/ST) which increased by decreasing the molecular weight of the UP or by decreasing the molecular weight of the LPA [16], leading belatedly to a phase separation. Pore formation was then not favored in the highly connected network, which was consistent with the high volume shrinkage (>7%) reported for these samples. An important stress was then generated throughout the sample, leading to strong deformations at the surface which created the observed holes. This phenomenon was not likely to occur with

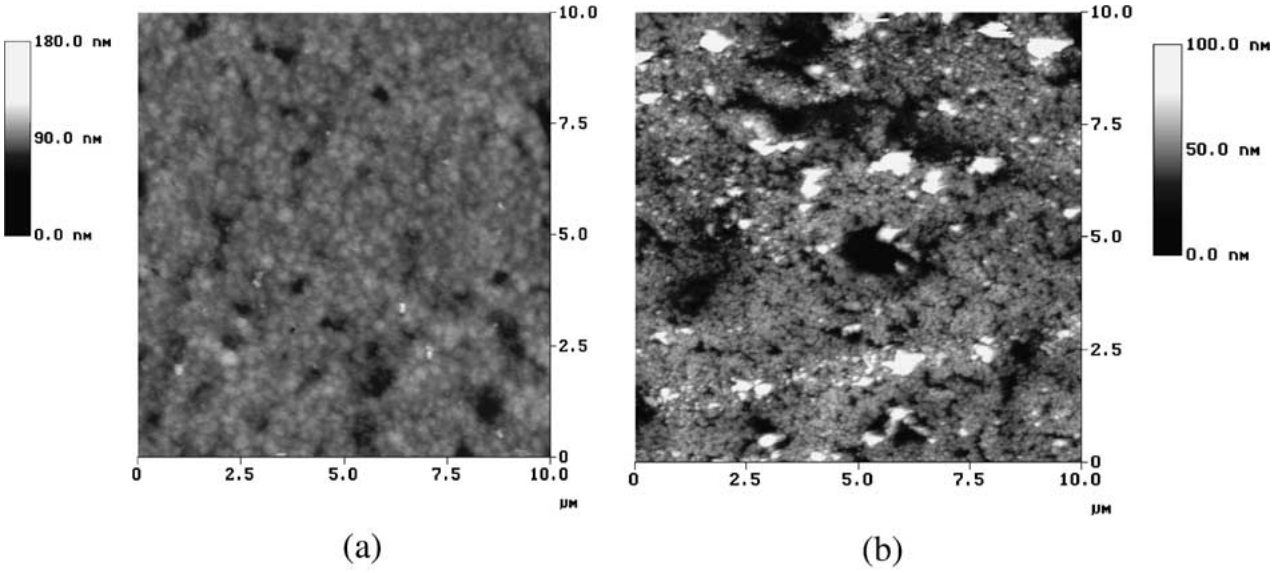

Figure 5 AFM images of (a) BMC2 surface and (b) TB2 surface.

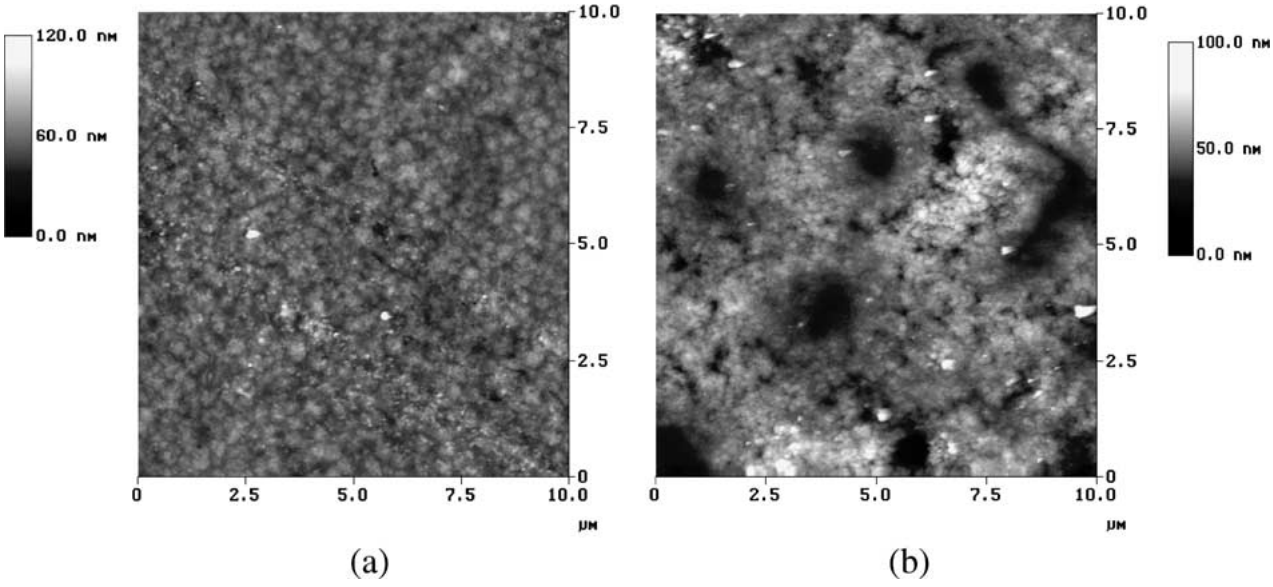

Figure 6 AFM images of (a) BMC3 surface and (b) TB3 surface.

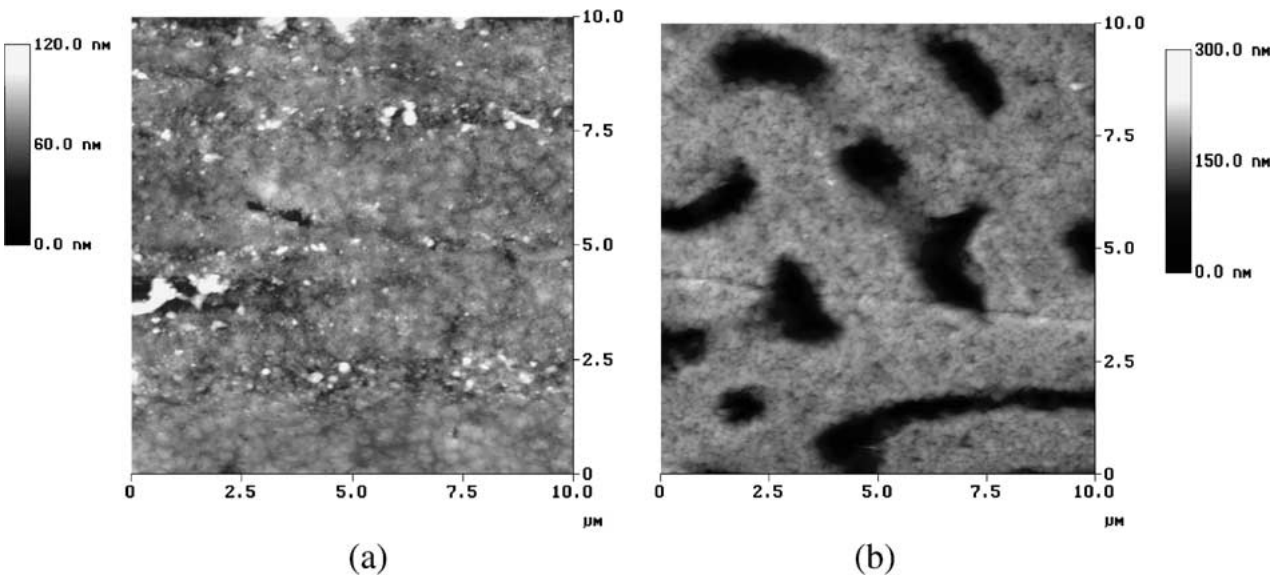

Figure 7 AFM images of (a) BMC4 surface and (b) TB4 surface.

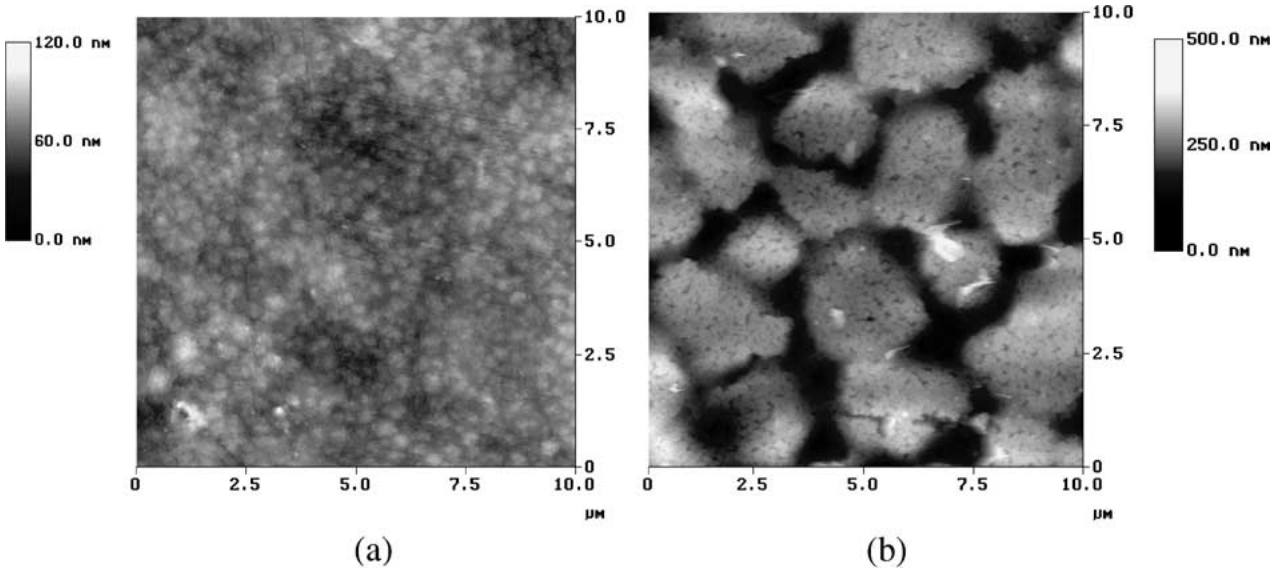

Figure 8 AFM images of (a) BMC5 surface and (b) TB5 surface.

increased LPA molecular weight (compositions 2 and 3). The miscibility domain of the considered ternary blends decreased leading to a precocious phase separation and consequently to a less connected polymeric network where formation of pores was favored (confirmed by the lower shrinkage volume and higher pore volume reported in Table IV). These observations illustrated the necessity for a polymerization shrinkage compensation mechanism to relax the stress inside the bulk by pores formation.

For BMC, an homogeneous discontinuous structure (with particles linked together to form aggregates randomly disposed at the sample surface) was observed whatever the molecular weight of LPA was considered. Corresponding measured roughnesses were low and constant (ranging between 5 and 8 nm), in contrast with results reported for TB. This was explained by the shrinkage compensation which occured even in the case of low molecular weight LPA due to the presence of fillers and fibers that favored phase separation and consequently pores formation. Stress relaxation occurred then in the bulk, leading to the absence of surface deformation (hole) that accounted for the high roughness reported before. The resulting BMC surface morphology was then not highly dependent with the LPA molecular weight. This result confirmed the key-role of fillers in the shrinkage compensation of BMC during industrial proceedings, generally not considered in most of the studies.

3.2.2. Influence of the amount of LPA

For a same type of LPA ($M_n = 2250$ g $\cdot$ mol^{-1}) the influence of the amount of LPA is illustrated by AFM images of compositions 3 and 6 (respectively 18 and 12% of LPA) (Fig. 6 and 9). A higher amount of LPA led to a larger pores volume (corresponding to a smaller shrinkage) either for the TB or the BMC, leading consequently to a higher roughness. The variations were however more significant in the case of the TB.

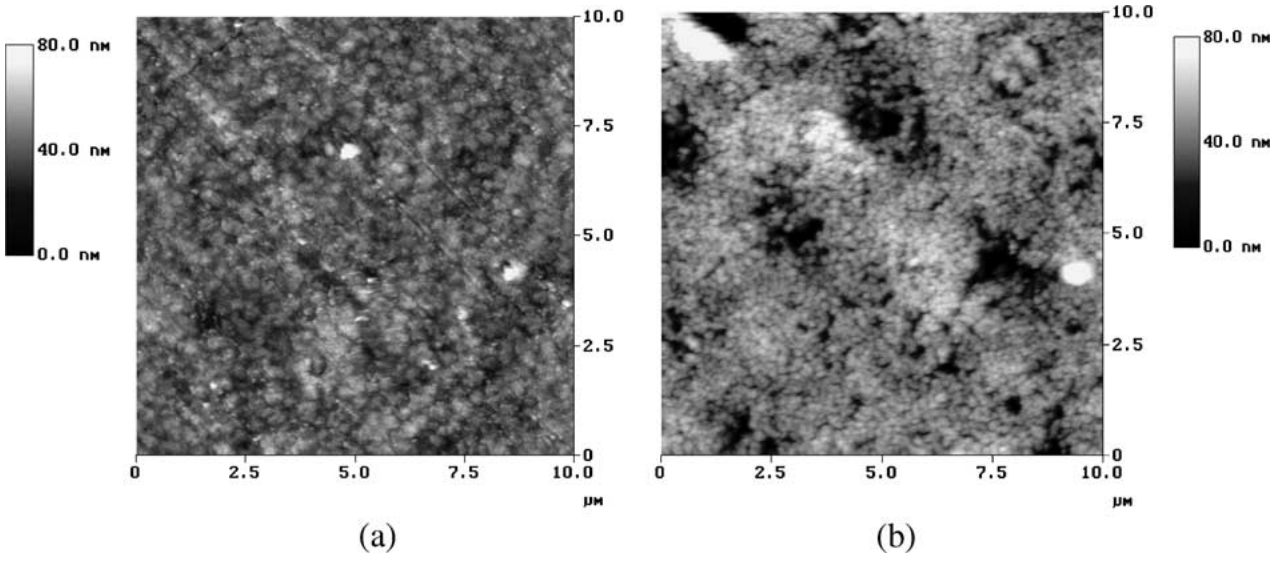

Figure 9 AFM images of (a) BMC6 surface and (b) TB6 surface.

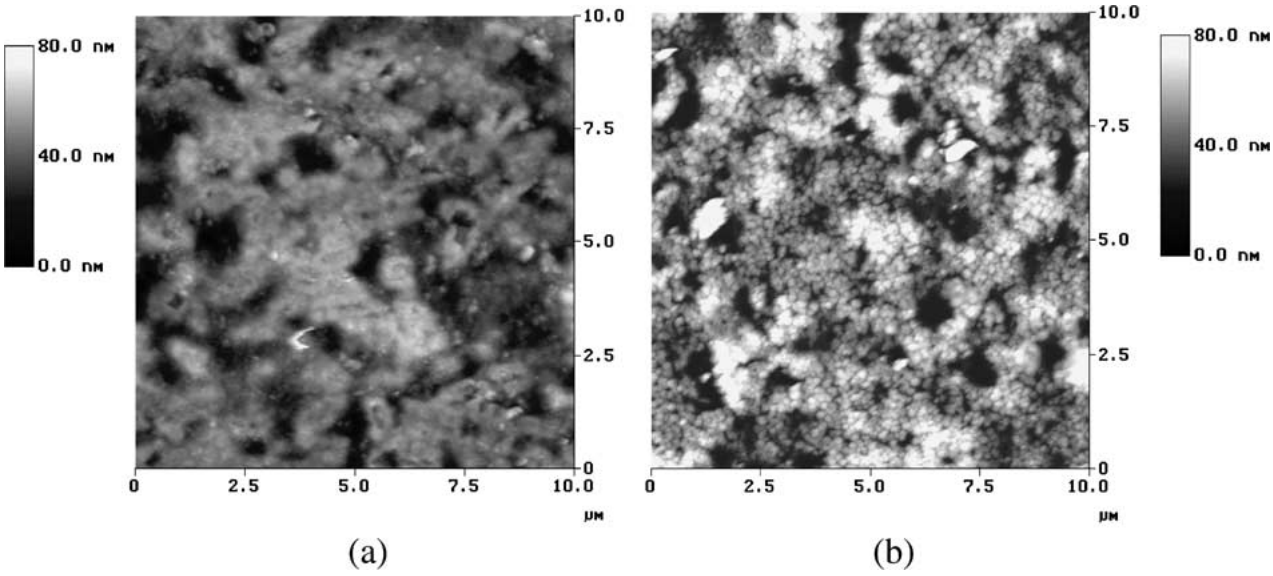

Figure 10 AFM images of (a) BMC7 surface and (b) TB7 surface.

3.2.3. Influence of the chemical nature

For a constant concentration of LPA (12 wt%), we studied the influence of the chemical nature of the LPA (saturated polyester and urethane modified saturated polyester). It has been reported that urethane modified saturated polyester exhibit lower miscibility with UP/styrene blends [17]. This can be explained by the chemical modification of the LPA (due to the presence of the urethane function) but also by the increased molecular weight (5300 $g \cdot mol^{-1}$).

In the case of the composition 7 (urethane modified LPA), AFM image showed an heterogeneous structure in TB and BMC with aggregates and holes presenting various sizes, randomly disposed all other the surface (Fig. 10). Aggregates were clearly visible and constituted a loose network with many small holes. This morphology led to a high roughness and could be correlated to the high pore volume measured for the samples. This was compared with composition 6 (saturated polyester) characterized by a more connected network, with less and smaller holes at surface, and a lower pores volume in the bulk. The corresponding BMC presented an homogeneous surface, with aggregates well dispersed all over the surface. The comparison of the morphologies of these two compositions was consistent with the lower miscibility of the considered urethane modified LPA which provoked a precocious phase separation, and consequently a looser network where pores formation was favored. In this particular case, one observed a good correlation between the surface roughness of TB and BMC: an increased roughness of the TB led to an increased roughness of the BMC.

Despite the presence of holes and aggregates, the morphology of composition 7 was drastically different that the one observed for a low molecular weight LPA where holes size was bigger, aggregates size smaller and network more connected (Fig. 8). It is important to note that for these two compositions (5 and 7), the origin of the holes at surfaces was completely different. In one case (low molecular weight LPA—composition 5) the holes originated from strong deformations of the surface due to intensive volume shrinkage. In the other case (urethane modified LPA—composition 7), holes resulted directly from the high pore volume generated in the structure.

4. Conclusion

Surfaces of miscible thermoset blends and of the corresponding BMC were compared by AFM. BMC and TB surfaces were constituted by aggregates linked together apart from TB without LPA. The discontinuous nature of these surfaces implied a phase separation at the surface during cross-linking. TB surface morphology (aggregates size and arrangement) and roughness were governed by the initial miscibility and its evolution during cross-linking. BMC surfaces reflected the morphology and the roughness of the TB surface. However, when the LPA molecular weight was too low to allow the development of pores inside the bulk, large holes were observed at TB surface. The BMC did not present such holes since pores could be developed inside the bulk with the help of fillers.

A good shrinkage control needed a large pore volume that corresponded to a rough surface of BMC since some pores could intercept the surface. Surface aspect and shrinkage control were then opposite properties, for which a comprise should be found.

Acknowledgment

The authors thank A. Richard for SEM and Menzolit company for their financial support and their active contribution to this work.

References

1. J. L. LUCAS, J. BORRAJO and R. J. J. WILLIAMS, *Polymer* **34** (1993) 1886.
2. K. W. LEM and C. D. HAM, *J. Appl. Polym. Sci.* **28** (1983) 3185.
3. M. KINKELARR, B. WANG and L. J. LEE, *Polymer* **35** (1994) 3011.

4. Y. J. HUANG and C. C. SU, *J. Appl. Polym. Sci.* **55** (1995) 323.
5. J. P. LECOINTE, J. P. PASCAULT, L. SUSPENE and Y. S. YANG, *Polymer* **33** (1992) 3226.
6. Y. J. HUANG and C. M. LIANG, *ibid.* **37** (1996) 401.
7. W. LI and J. LEE, *ibid.* **39** (1998) 5677.
8. M. B. CHAN-PARK and F. J. MC GARRY, *J. Adv. Mat.* **27** (1995) 47.
9. Z. ZHANG and S. ZHU, *Polymer* **41** (2000) 3861.
10. C. SERRÉ, M. VAYER, C. OLLIVE and R. ERRE, *J. Mater. Sci*. **34** (1999) 4203.
11. C. SERRÉ, M. VAYER, N. BOYARD and R. ERRE, *ibid.* **36** (2001) 113.
12. C. SERRÉ, Thesis, University of Orleans, France, 2000.
13. N. DESLANDES, V. BELLENGER, F. JAFFIOL and J. VERDU, *Composites* **29A** (1998) 1481.
14. M. F. VALLAT, J. SCHULTZ, C. MAUZAC and M. JACQUIN, *Polym. Adv. Technol.* **10** (1999) 237.
15. L. SUSPENE, D. FOURQUIER and Y. S. YANG, *Polymer* **32** (1991) 1593.
16. Y. J. HUANG and W. C. JIANG, *ibid.* **39** (1998) 6631.

Received 9 March
and accepted 18 December 2001